JOURNAL OF GUIDANCE, CONTROL, AND DYNAMICS
Vol. 20, No. 1, January–February 1997

Orbital Maneuvers via Feedback Linearization and Bang–Bang Control

Sanguk Lee
Electronics and Telecommunications Research Institute, Taejon 305-600, Republic of Korea
and
J. E. Cochran Jr.
Auburn University, Auburn, Alabama 36849-5338

Spacecraft orbital maneuver problems are treated using feedback linearization and sliding mode control. The nonlinear dynamic system representing the two-body system of a spacecraft and primary gravitational source is transformed into a linear controllable one by feedback linearization, then thrust-coast-thrust type control laws are found by using optimal linear tracking and time-varying Riccati equations. Bang–bang type control laws for orbital maneuvers of spacecraft are obtained by using a sliding mode control scheme. Special two-body orbits, obtained by solving Lambert's problem in which impulsive changes in velocity are assumed possible for each orbital maneuver problem, are used as desired trajectories. However, initial and final control efforts are bounded in magnitude. This approach quickly produces very reasonable results in terms of total ΔV that are close to the impulsive solutions to these two-point boundary-value problems.

I. Introduction

An orbital maneuver, defined as a change in the shape and/or orientation of an orbit, may be carried out using natural and/or artificial perturbations. For more than three decades, many researchers have sought to determine optimal orbital maneuvers in many different ways. The problem of optimizing finite-thrust spacecraft trajectories has been solved using direct and indirect methods. In the direct parameter optimization method, the continuous control is approximated by a sequence of constant parameters. The solution of such an optimization problem requires mathematical programming, either linear or nonlinear, to obtain a solution. On the other hand, indirect methods based on the necessary conditions for optimality from the calculus of variations result in two-point boundary-value problems (TPBVPs) that also must be solved numerically except for especially simple cases.

Regarding indirect methods as applied to orbit transfer, extensive theoretical work was done by Lawden.[1] He introduced the famous primer vector theory for trajectory optimization for space navigation. The resulting TPBVP is very hard to solve for some problems due to its sensitivity to the initial guesses of costate variables. Kelly[2] solved this type of TPBVP by using a gradient method. The shooting method was used by Melbourn,[3] Handelsman,[4] and Lion et al.[5] to solve TPBVPs. Trajectory optimization problems based on linearized system equations have been solved by Euler[6] and Tapley and Fowler[7] and are used in terminal guidance. McCue[8] and Lewallen[9] used a quasilinearization method to solve the more difficult nonlinear trajectory problem. Recently, Dickmanns and Well[10] introduced a collocation method using Hermite cubics in which they convert the optimal control problem into a nonlinear programming problem. Hargraves and Paris[11] developed this idea for a direct method,

Sanguk Lee is a member of the senior research staff at the Electronics and Telecommunications Research Institute (Telemetry Tracking and Commands Section, Satellite Communications Division) in Korea. He received his M.S. and Ph.D. in Aerospace Engineering from Auburn University in 1991 and 1994, respectively. His research interests include dynamics and control of spacecraft. He is a member of AIAA, the Korean Society for Aeronautical and Space Sciences, the Institute of Control, Automation and Systems Engineers, and the Korean Space Science Society.

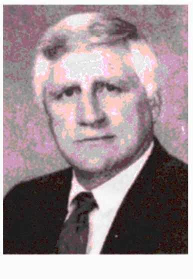

John E. Cochran Jr. received his B.A.E. and M.S. from Auburn University in 1966 and 1967, respectively, and his Ph.D. from the University of Texas at Austin in 1970. He also received a J.D. from Jones Law Institute in 1976. He has been a member of the Auburn University faculty since 1969 and is currently Professor and Head of the Department of Aerospace Engineering. He is an Associate Fellow of AIAA.

Presented as Paper 94-3749 at the AIAA/AAS Astrodynamics Conference, Scottsdale, AZ, Aug. 1–3. 1994; received Aug. 21, 1995; revision received July 29, 1996; accepted for publication Aug. 12, 1996. Copyright © 1996 by the American Institute of Aeronautics and Astronautics, Inc. All rights reserved.

and Enright and Conway[12] extended the method to solve trajectory optimization problems for spacecraft. Hodges and Bless[13] developed a weak Hamiltonian finite element method, and Hodges et al.[14] applied it to solve an atmospheric flight trajectory optimization problem.

Although not extremely complex, the orbital maneuver problem still requires nonlinear optimization. One approach to finding solutions to such problems is feedback linearization, a technique of transforming a nonlinear system into an equivalent, controllable linear form by using nonlinear state and feedback transformations. The theoretical basis was developed by Isidori et al.[15] and Hunt et al.,[16] building on Krener's[17] solution to the linearization problem with only a local change of coordinates in the state space. It was applied successfully to a helicopter autopilot problem by Meyer et al.[18] It also has been applied to solve problems involving robot arm manipulation, aircraft dynamics, and electric motor control. Dwyer[19,20] used this method to exactly solve two nonlinear control problems of large-angle rotational maneuvers with external torque and momentum exchange, respectively. Recently, Van Buran and Mease[21] solved an aerospace plane guidance problem by using this feedback linearization.

In previous related work,[22] a new approach based on advanced nonlinear control theory was introduced to solve orbital transfer problems. The nonlinear dynamic system representing the two-body system of a spacecraft and primary gravitational source was transformed into a linear controllable one by feedback linearization described in the next section. In other words, the authors reduced the problem to that of solving a linear control problem with dynamics defined by a pair of double integrators. Linear optimal tracking solutions were obtained by using a Lambert orbit as reference trajectory. Here, Lambert orbit means a two-body, or Keplerian, orbit obtained by solving Lambert's problem.[23] Also, orbit means any two-body orbit. Furthermore, trajectory refers to the path of the spacecraft when thrusting and coasting. Then, the solutions were transformed back into nonlinear ones by inversion of nonlinear input transformations. This method does not produce bang–bang type control, but it gives thrust-coast-thrust type control.

Another method for handling the nonlinear control problem is sliding mode control. This is a type of variable structure control utilizing a high-speed switching control law to drive a nonlinear system state trajectory onto a user-chosen surface, the so-called sliding surface, and to maintain the system state trajectory on the sliding surface at subsequent times. The concept of a sliding surface was introduced by Filippov.[24] The sliding mode control scheme allows for system parameter uncertainty and unmodeled dynamics. However, this technique has limits on its practicability, such as chattering and large control effort when tracking performance requirements are tight. Both these limitations may be minimized by employing a boundary layer[25] as a margin. Also, we can trade off tracking performance for more reasonable control effort.

In this paper, another approach based on sliding mode control is used to solve orbital maneuver problems without employing the calculus of variations. Bang–bang type solutions to orbital maneuvers obtained by employing sliding mode control with bounded control effort are presented. Undesirable chattering phenomena have been removed by introducing the boundary-layer concept.

We first describe the model used. Second, we provide a short section on feedback linearization. Third, we review Lambert's theorem. Fourth, we briefly describe sliding mode control. This is followed by examples of the use of feedback linearization and sliding mode control.

II. Equations of Motion

The dynamic model chosen for this work includes a satellite that moves under the influence of the Earth's gravitational field and a variable thrust acceleration. Both the Earth and satellite are modeled as point masses.

A two-dimensional formulation is given here, but the methods described are applicable to three-dimensional problems as well. As shown in Fig. 1, the two-dimensional inertial coordinate system OXY, with origin at the center of the Earth, is used as the basic reference coordinate system. The well-known equations of motion governing a satellite thrusting in an inverse-square gravitational field in terms of local polar coordinates are

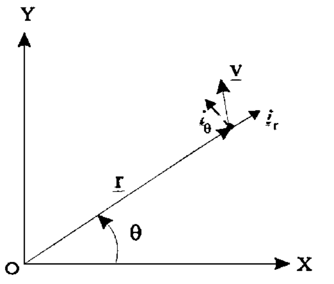

Fig. 1 Motion of satellite in polar coordinate system.

$$\ddot{r} - r\dot{\theta}^2 = -(\mu/r^2) + u_r \tag{1}$$

$$r\ddot{\theta} + 2\dot{r}\dot{\theta} = u_\theta \tag{2}$$

where r is the radial distance from the gravitational center at O to the spacecraft at S, θ is the polar angle, and μ is the gravitational parameter.

We can write the equations of motion in the vector form,

$$\dot{\boldsymbol{x}} = \boldsymbol{f}(\boldsymbol{x}) + g(\boldsymbol{x})\boldsymbol{u} \tag{3}$$

where $\boldsymbol{x} = [x_1, x_2, x_3, x_4]^T = [r, \theta, \dot{r}, \dot{\theta}]^T$ and $\boldsymbol{u} = [u_1, u_2]^T = [u_r, u_\theta]^T$.

III. Lambert's Theorem

For the two-body TPBVP, Lambert[23] gave a remarkable theorem that the orbital transfer time depends only on the semimajor axis of the transfer orbit, the sum of the distances r_1 and r_2 of the initial and final points, p_1 and p_2, respectively, from O, and the length of the chord joining these points, i.e.,

$$\sqrt{\mu}(t_2 - t_1) = F(a, r_1 + r_2, c) \tag{4}$$

where $t_2 - t_1$ is the time required for the orbiting body to coast from p_1 to p_2. The geometrical configuration associated with Lambert's problem is shown in Fig. 2.

Lambert's theorem[26] can be expressed more specifically as

$$\sqrt{\mu}(t_2 - t_1) = a^{\frac{3}{2}}[(\xi - \sin\xi) - (\zeta - \sin\zeta)] \tag{5}$$

where a is the semimajor axis of the transfer orbit and ξ and ζ are variables defined as

$$\xi = 2\sin^{-1}(\sqrt{\gamma/2a}) \quad \text{and} \quad \zeta = 2\sin^{-1}[\sqrt{(\gamma - c)/2a}] \tag{6}$$

In Eq. (6), $\gamma = \frac{1}{2}(r_1 + r_2 + c)$ is the semiperimeter of the triangle Op_1p_2.

For a given transfer time Δt, orbital elements may be obtained by using Lambert's theorem. The semimajor axis can be obtained by solving the equation

$$f(a) = \sqrt{\mu}\Delta t - a^{\frac{3}{2}}[(\xi - \sin\xi) - (\zeta - \sin\zeta)] = 0 \tag{7}$$

An efficient way to solve Eq. (7) is with a Newton–Raphson iterative method. For the Newton–Raphson method,

$$a_{i+1} = a_i - \frac{f(a_i)}{f'(a_i)} \tag{8}$$

Once the semimajor axis has been found, the eccentricity of the transfer orbit may be calculated from

$$e^2 = 1 - 4\frac{(\gamma - r_1)(\gamma - r_2)\sin^2[(\xi + \zeta)/2]}{c^2} \tag{9}$$

Next, the true anomalies at the ends of the chord may be obtained by using the familiar orbit equation,

$$r = \frac{a(1 - e^2)}{1 + e\cos\nu} \tag{10}$$

where ν is the true anomaly.

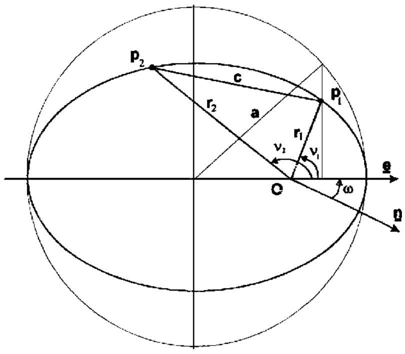

Fig. 2 Geometry of Lambert's problem.

The initial velocity vector can be found by using standard formulas (see, for example, Ref. 23, p. 126) and the reference trajectories can be generated.

IV. Feedback Linearization

As already mentioned, feedback linearization is the technique of transforming a controllable nonlinear system into an equivalent, controllable, linear form by using state and feedback transformations. The actual system and controller remain nonlinear. References 25 and 26 provide detailed theoretical background on feedback linearization. For the sake of completeness, we give some mathematics that is needed in understanding the technique.

For a single-input/single-output (SISO) nonlinear system of the form

$$\dot{\boldsymbol{x}} = \boldsymbol{f}(\boldsymbol{x}) + \boldsymbol{g}(\boldsymbol{x})u \tag{11}$$

$$y = h(\boldsymbol{x}) \tag{12}$$

where the vector functions $\boldsymbol{f}: R^n \to R^n$ and $\boldsymbol{g}: R^n \to R^n$ are C^∞ vector fields; $h: R^n \to R^n$ is a C^∞ scalar function; and the Lie derivative of $h(\boldsymbol{x})$ along the direction of vector $\boldsymbol{f}(\boldsymbol{x})$ is a scalar function defined as

$$L_f h = \nabla h \cdot \boldsymbol{f} \tag{13}$$

The Lie derivative may be taken recursively:

$$L_f^0 h = h, \qquad L_f^i h = L_f\left(L_f^{i-1} h\right) = \nabla\left(L_f^{i-1} h\right) \cdot \boldsymbol{f} \qquad \text{for} \quad i = 1, 2, \ldots \tag{14}$$

The Lie bracket of $\boldsymbol{f}$ and $\boldsymbol{g}$ is a third vector field defined as

$$[\boldsymbol{f}, \boldsymbol{g}] = \nabla \boldsymbol{g} \cdot \boldsymbol{f} - \nabla \boldsymbol{f} \cdot \boldsymbol{g} \tag{15}$$

The Lie bracket $[\boldsymbol{f}, \boldsymbol{g}]$ is usually written as $ad_f \boldsymbol{g}$. The Lie bracket may be defined recursively by

$$ad_f^0 \boldsymbol{g} = \boldsymbol{g}, \qquad ad_f^i \boldsymbol{g} = \left[\boldsymbol{f}, ad_f^{i-1} \boldsymbol{g}\right] \quad \text{for} \quad i = 1, 2, \ldots \tag{16}$$

Consider a SISO nonlinear system in Eqs. (11) and (12) with dimension n. There exists an output function $h(\boldsymbol{x})$ with relative degree κ at a point $\boldsymbol{x}_0$ if and only if the following conditions are satisfied:

rank$(ad_f^i \boldsymbol{g}) = \kappa$ and distribution (Δ) is involutive near $\boldsymbol{x}_0$, where

$$\text{rank}(ad_f^i \boldsymbol{g}) = \left[\boldsymbol{g}(\boldsymbol{x}_0), ad_f \boldsymbol{g}(\boldsymbol{x}_0), ad_f^{\kappa-1} \boldsymbol{g}(\boldsymbol{x}_0)\right] \tag{17}$$

$$\Delta = \text{span}\left\{\boldsymbol{g}(\boldsymbol{x}), ad_f \boldsymbol{g}(\boldsymbol{x}_0), \ldots, ad_f^{\kappa-2} \boldsymbol{g}(\boldsymbol{x})\right\} \tag{18}$$

The relative degree κ is characterized as the number of times one has to differentiate the output function to have the input u appear explicitly. If there exists an output function $h(\boldsymbol{x})$ with relative degree κ and the dimension n is equal to the relative degree, then the system is fully feedback linearizable.

The idea of relative degree can be extended to multi-input/multi-output (MIMO) nonlinear systems of the form

$$\dot{\boldsymbol{x}} = \boldsymbol{f}(\boldsymbol{x}) + g(\boldsymbol{x})\boldsymbol{u} \tag{19}$$

$$\boldsymbol{y} = \boldsymbol{h}(\boldsymbol{x}) \tag{20}$$

where $\dot{\boldsymbol{x}}$ and $\boldsymbol{f}(\boldsymbol{x})$ are $n \times 1$ vectors; $g(\boldsymbol{x})$ is $n \times m$; and $\boldsymbol{y}$, $\boldsymbol{h}(\boldsymbol{x})$, and u are $m \times 1$ vectors. The MIMO nonlinear system of the form of Eqs. (19) and (20) has a set of relative degrees κ at a point $\boldsymbol{x}_0$ if

$$L_{g_j} L_f^{k_i - 1} h_i(\boldsymbol{x}) = 0 \tag{21}$$

for all $1 \leq j \leq m$, for all $1 \leq i \leq m$, for all $k_i \leq \kappa_i - 1$, and for all $\boldsymbol{x}$ in a neighborhood of $\boldsymbol{x}_0$ and the $m \times m$ matrix,

$$E(\boldsymbol{x}) = \begin{bmatrix} L_{g_1} L_f^{k_1-1} h_1(\boldsymbol{x}) & \cdots & L_{g_m} L_f^{k_1-1} h_1(\boldsymbol{x}) \\ L_{g_1} L_f^{k_2-1} h_2(\boldsymbol{x}) & \cdots & L_{g_m} L_f^{k_2-1} h_2(\boldsymbol{x}) \\ \cdots & \cdots & \cdots \\ L_{g_1} L_f^{k_m-1} h_m(\boldsymbol{x}) & \cdots & L_{g_m} L_f^{k_m-1} h_m(\boldsymbol{x}) \end{bmatrix} \tag{22}$$

is nonsingular at $\boldsymbol{x}_0$. The matrices (17) and (22) are equivalent to the controllability matrix $\{B, AB, \ldots, A^{n-1}B\}$ in linear control theory.

The feedback linearization procedure can be summarized as follows:

$$\begin{gathered} \dot{\boldsymbol{x}} = \boldsymbol{f}(\boldsymbol{x}) + g(\boldsymbol{x})\boldsymbol{u} \xrightarrow[z = \Psi(x)]{u = \alpha(x) + \beta(x)\nu} \dot{z} = Az + B\boldsymbol{\nu} \\ \boldsymbol{y} = \boldsymbol{h}(\boldsymbol{x}) \end{gathered} \tag{23}$$

The nonlinear equations that describe the system should have the form of Eq. (19) if the system is to be transformed into a controllable linear one by using feedback linearization. If we obtain a proper nonlinear change of state variables defined by $\boldsymbol{\Psi}(\boldsymbol{x})$, a nonlinear feedback function $\boldsymbol{\alpha}(\boldsymbol{x})$, and a linear invertible change of coordinates in the input $\beta(\boldsymbol{x})$ such that the input/output behavior of the system is linear and controllable, then Eq. (19) can be transformed into the form

$$\dot{z} = Az + B\boldsymbol{\nu} \tag{24}$$

where z and $\boldsymbol{\nu}$ are new state and control variables, respectively, and A and B are the constant system and control matrices, respectively. This type of transformation is exact, and the control obtained from the system is directly applicable to the nonlinear system without any internal modifications.

For the mathematical model in hand, the output relation $\boldsymbol{y} = \boldsymbol{h}(\boldsymbol{x})$ is selected as the position vector and we assume that all position variables are fully observable. The relative degrees of the system are $\{2, 2\}$, i.e., the sum of relative degrees $\kappa = 4$, which is equal to the system dimension. Therefore, the model is fully feedback linearizable. A matrix form of the equations of motion, which is the canonical form for feedback linearization, is

$$\dot{z}_1 = z_2; \qquad \dot{z}_2 = \boldsymbol{f}_2(z_1, z_2) + g_2(z_1, z_2)\boldsymbol{u} \tag{25}$$

where $z_1 = [r, \theta]^T$; $z_2 = [\dot{r}, \dot{\theta}]^T$.

If we define a new control variable,

$$\boldsymbol{\nu} = \boldsymbol{f}_2(z_1, z_2) + g_2(z_1, z_2)\boldsymbol{u} \tag{26}$$

then, we may reduce Eqs. (25) to

$$\dot{z}_1 = z_2, \qquad \dot{z}_2 = \boldsymbol{\nu} \tag{27}$$

The input transformation is

$$\boldsymbol{u} = -g_2(z_1, z_2)^{-1} \boldsymbol{f}_2(z_1, z_2) + g_2(z_1, z_2)^{-1} \boldsymbol{\nu} \tag{28}$$

and the state transformation is

$$z = \boldsymbol{\Psi}(\boldsymbol{x}) = \boldsymbol{x} \tag{29}$$

where $g_2(z_1, z_2)$ should not be singular.

We can write Eqs. (27) explicitly in the so-called Brunovsky canonical form,

$$\dot{z} = Az + B_2 v = \begin{bmatrix} 0 & I \\ 0 & 0 \end{bmatrix} \begin{bmatrix} z_1 \\ z_2 \end{bmatrix} + \begin{bmatrix} 0 \\ I \end{bmatrix} \begin{bmatrix} v_1 \\ v_2 \end{bmatrix} \tag{30}$$

where $z = [z_1^T, z_2^T]^T$.

V. Sliding Mode Control

Sliding mode control[24] is introduced to allow for model inaccuracy that may come from actual uncertainty about the system due to unknown system parameters or from the purposeful choice of a simplified model for the dynamic system. Neglecting the Earth's oblateness is an example of the latter. The sliding controller design provides a systematic approach to the problem of maintaining system stability and consistent performance in the presence of such uncertainties. However, these methods sometimes require high control effort. Therefore, we may need a trade-off between tracking performance and power requirements.

Sliding mode control is often discussed in connection with an nth-order nonlinear system. Consider, as an example, the single-input dynamic system

$$x^{(n)} = f(\boldsymbol{x}) + b(\boldsymbol{x})u \tag{31}$$

where $\boldsymbol{x} = [x, \dot{x}, \ldots, x^{(n-1)}]^T$. The control problem is to make the state $\boldsymbol{x}$ track a desired time-varying state trajectory defined by $\boldsymbol{x}_d = [x_d, \dot{x}_d, \ldots, x_d^{(n-1)}]^T$ in the presence of model imprecision on $f(\boldsymbol{x})$ and $b(\boldsymbol{x})u$. Let the tracking error vector be

$$\tilde{\boldsymbol{x}} = \boldsymbol{x} - \boldsymbol{x}_d = \left[\tilde{x}, \dot{\tilde{x}}, \ldots, \tilde{x}^{(n-1)}\right]^T \tag{32}$$

Also, let us define a time-varying sliding surface $s(\boldsymbol{x}, t)$ by

$$s(\boldsymbol{x}, t) = \left(\frac{\mathrm{d}}{\mathrm{d}t} + \lambda\right)^{n-1} \tilde{x} = 0 \tag{33}$$

where λ is a positive constant. Then the sliding condition

$$\frac{1}{2}\frac{\mathrm{d}}{\mathrm{d}t}s^2 \leq -\eta|s| \tag{34}$$

where η is a positive constant that can be obtained from Lyapunov's stability theory.

Because our system is second order, let us consider, for the purpose of illustration, the scalar second-order system

$$\ddot{x} = f + bu \tag{35}$$

where f and b may be functions of x and $\dot{x}$.

We assume that the system dynamics defined by f and the control gain b are not known exactly but may be estimated as $\hat{f}$ and $\hat{b}$, respectively. Then, the estimation error on f is assumed to be bounded by some known function $F = F(x, \dot{x})$, such that

$$|\hat{f} - f| \leq F \tag{36}$$

and $\hat{b}$ can be the geometric mean of minimum and maximum values of b. We may define a sliding surface $s(\boldsymbol{x}, t) = \dot{\tilde{x}} + \lambda\tilde{x} = 0$ and a desired trajectory $x(t) = x_d(t)$ for the system to track. We then have

$$\dot{s} = \ddot{x} - \ddot{x}_d + \lambda\dot{\tilde{x}} = f + bu - \ddot{x}_d + \lambda\dot{\tilde{x}} \tag{37}$$

The best estimation to a continuous control law that achieves $\dot{s} = 0$ is[25]

$$\hat{u} = \frac{-\hat{f} + \ddot{x}_d - \lambda\dot{\tilde{x}}}{\hat{b}} \tag{38}$$

To satisfy the sliding condition (34) in the presence of uncertainty in the dynamics f, we add a discontinuous term across the sliding surface $s = 0$ to get

$$u = \hat{u} - k\,\mathrm{sgn}(s) \tag{39}$$

From the sliding condition, we have

$$k = F + \eta \tag{40}$$

The presence of modeling imprecision and of disturbances often leads to chattering that is discontinuous across $s(\boldsymbol{x}, t)$. This can be eliminated by smoothing out the discontinuity in a boundary layer neighboring the switching surface. We let Φ be a prescribed function of time or a constant value and put

$$s(\boldsymbol{x}, t) \leq \Phi, \qquad \Phi > 0 \tag{41}$$

Then, we can rewrite Eq. (39) as

$$u = \hat{u} - k\,\mathrm{sgn}(s/\Phi) \tag{42}$$

This procedure can be easily extended to our system. That is, we may write

$$\ddot{\boldsymbol{x}} = \boldsymbol{f}(\boldsymbol{X}) + B(\boldsymbol{X})\boldsymbol{u} \tag{43}$$

where

$$\boldsymbol{x} = [r, \theta]^T, \qquad \boldsymbol{u} = [u_r, u_\theta]^T, \qquad \boldsymbol{X} = [r, \theta, \dot{r}, \dot{\theta}]^T$$

$$\boldsymbol{f}(\boldsymbol{X}) = \begin{bmatrix} r\dot{\theta}^2 - (\mu/r^2) \\ -(2\dot{r}\dot{\theta}/r) \end{bmatrix}, \qquad \text{and} \qquad B(\boldsymbol{X}) = \begin{bmatrix} 1 & 0 \\ 0 & 1/r \end{bmatrix}$$

Then, we may define λ, κ, η, and Φ. In the following section, we give two examples in which this technique is applied.

VI. Results

The two examples chosen are 1) an orbital maneuver between two coplanar, low-Earth circular orbits and 2) an apogee kick firing maneuver of a communications satellite from a transfer orbit to the geostationary orbit. For each example, the problem is to find the trajectories and control laws that require reasonable total ΔV obtained by integrating the total thrust accelerations.

The maneuver time is the same as the coasting time required to reach the final polar angle in an intermediate orbit. The intermediate orbit was taken as the average of the initial and final circular orbits for the low Earth orbit maneuver and as the final orbit for the geostationary transfer orbit maneuver.

The boundary conditions of the first example in the local polar coordinate system and the corresponding Lambert orbit for the given time are given in Table 1. The Lambert orbit has relatively small eccentricity. It is a coasting trajectory that connects two given spatial points. As used here, it satisfies the desired geometric boundary conditions, but not the boundary conditions on velocity.

Feedback Linearization Method

For a basis to use in comparing the results from different methods, we obtained a numerical solution to a nonlinear TPBVP, with no constraints on thrust acceleration as the control input. The performance index was chosen as an integral of the sum of the squares of the thrust acceleration components. Because the performance index

Table 1 Boundary conditions and Lambert orbit

Boundary conditions	Initial	Final
Radius r, km	6778.0	7378.0
Polar angle θ, rad	0	2.9496
Radial velocity $\dot{r}$, km/s	0	0
Angular rate $\dot{\theta}$, rad/s	1.1314×10^{-3}	9.9623×10^{-4}
Time, s	0	2782.0
Lambert orbit		*Orbital elements*
Semimajor axis, km		7078.0
Eccentricity		0.042581
Inclination, deg		0.0
Longitude of the ascending node, deg		Not defined
Longitude of argument of perigee, deg		−5.6684
True anomaly at $t = 0$, deg		5.6684
True anomaly at $t = 2782.026$, deg		174.64

is not the total ΔV required for a maneuver, these nonlinear results serve primarily as an order of magnitude standard for comparison.

An optimal linear tracking problem was solved using a Lambert orbit as the reference trajectory, so that the feedback linear system tracks the Lambert orbit. A performance index was chosen as

$$J = \frac{1}{2}[z(t_f) - z_{df}]^T S[z(t_f) - z_{df}] + \frac{1}{2}\int_{t_0}^{t_f} \left\{[z - z_d]^T Q[z - z_d] + \nu^T R\nu\right\} \mathrm{d}t \tag{44}$$

where z_d is the desired trajectory obtained by Lambert's theorem and S_f is a positive semidefinite matrix of weights on the final state error. Also, Q and R are a positive semidefinite weighting matrix on the state and a positive definite weighting matrix on the control, respectively. A time-varying Q matrix that weights the state variables in the performance index was used to obtain a control law with a thrust-coast-thrust shape and to avoid extremely steep peaks in commanded accelerations at both ends of the trajectory. The weighting matrices for the optimal linear tracking problem were selected as

$$Q(t) = \varepsilon(t) \times \mathrm{diag}[9 \times 10^{11}, 7.4 \times 10^{-16}, 3.53 \times 10^{-6}, 8.0 \times 10^{-5}]$$

$$S_f = \mathrm{diag}[1 \times 10^{-5}, 3 \times 10^{-7}, 0.7, 0.7], \qquad R = \mathrm{diag}[1, 1]$$

where a time-varying scalar function $\varepsilon(t)$ is shown in Fig. 3. As expected, the time histories of thrust acceleration show thrust-coast-thrust behavior (see Figs. 4 and 5) and those of the state variables show that the spacecraft enters the Lambert orbit and then leaves it and merges with the final orbit, as shown in Figs. 6 and 7. In these figures, NL indicates the nonlinear optimal control solution, FBL indicates the feedback linearization solution, and SLD indicates the sliding mode control solution.

Sliding Mode Control Method

A sliding mode control scheme using bounded thrust accelerations was also used to obtain a bang–bang type controller for the same two orbital maneuvers. The thrust accelerations for the first and second examples are bounded by the values of $\frac{1}{10}$ g and 1 g (9.8 m/s^2), respectively. The sliding surface was chosen such that $\boldsymbol{s}(\boldsymbol{x}, t) = \dot{\tilde{\boldsymbol{x}}} + \lambda\tilde{\boldsymbol{x}} = \boldsymbol{0}$. Table 2 contains the parameters used for sliding mode control.

The dynamic system at hand has the form of Eq. (43). It is assumed that $\boldsymbol{f}(\boldsymbol{X})$ and $B(\boldsymbol{X})$ are known exactly. In other words, Eq. (36) is always zero, and Eq. (40) is constant. The term sgn(s/Φ) was chosen as s/Φ, for $s/\Phi < 1$, to keep the system on or very near the sliding surface consistently. The reference trajectory used in the feedback linearization approach was again used. The bang–bang type time histories of the controller are shown in Fig. 4. The time histories of the components of thrust acceleration histories are presented in Fig. 5. Time histories of state variables are shown in Figs. 6 and 7. They rapidly merge into the values corresponding to the Lambert orbit, track those, and then merge into the final orbit. A comparison of the ΔV required is made in Table 3. Needless to say, impulsive solutions to Lambert's problem have minimum values. However, bang–bang type solutions with sliding mode control have values of ΔV very close to the impulsive solution and much closer than the feedback linearization or nonlinear solutions. Also, the thrust profile is more realistic for a space mission. Here, the ΔV for the Lambert's orbit transfer was obtained from the specified orbit geometry and ΔV determined from the integrals of the magnitudes of the respective thrust accelerations.

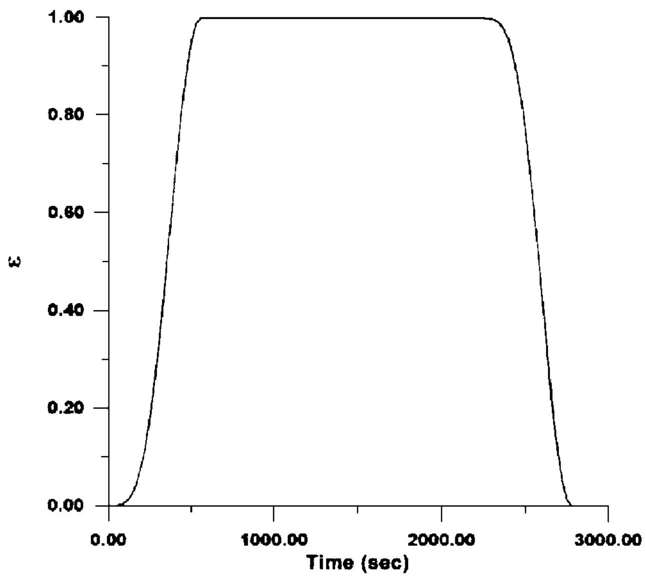

Fig. 3 Time history of scalar function $\varepsilon(t)$.

Table 2 Parameters

Parameters	Example 1	Example 2
λ_1	0.10	2.0
λ_2	0.053	0.20
η_1	7.0×10^{-4}	0.0043
η_2	4.5×10^{-5}	0.030
Φ_1	0.40	0.030
Φ_2	0.014	0.050

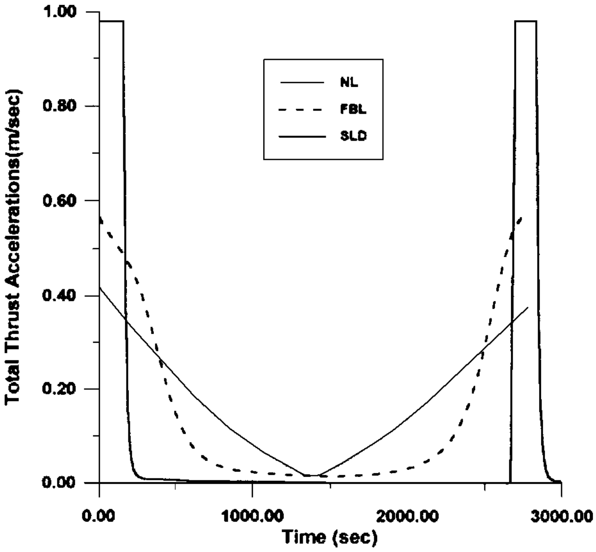

Fig. 4 Time histories of magnitude of thrust accelerations.

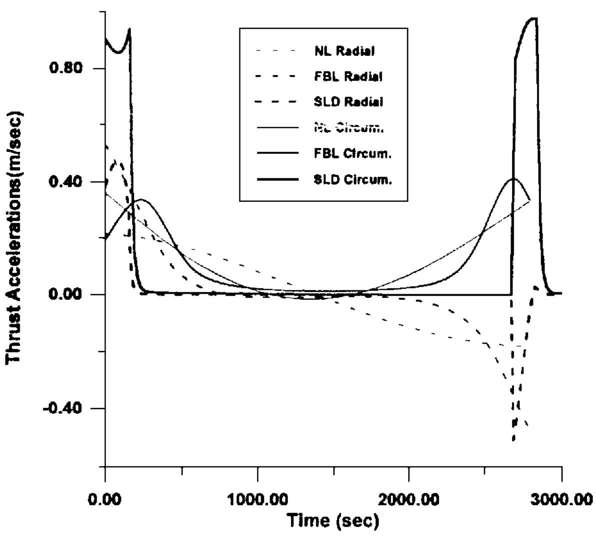

Fig. 5 Time histories of components of thrust accelerations.

Table 3 Total costs, ΔV for each method

Methods	ΔV, km/s
Lambert's problem (impulsive), LO	0.321066
Nonlinear optimal control, NL	0.489265
Feedback linearization method, FBL	0.430523
Sliding mode control method, SLD	0.338109

Table 4 Boundary conditions

	Initial	Final
Radius ΔV, km	42,164.0	42,164.0
Polar angle ΔV, deg	180.000	181.253
Radial velocity ΔV, km/s	0.0	0.0
Angular rate $\dot{\theta}$, rad/s	4.04763×10^{-5}	7.29212×10^{-5}
Time, s	0.0	200.000

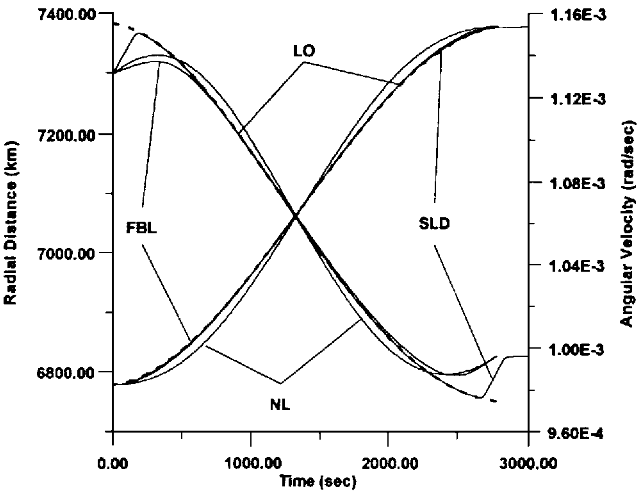

Fig. 6 Time histories of radial distance and angular velocity.

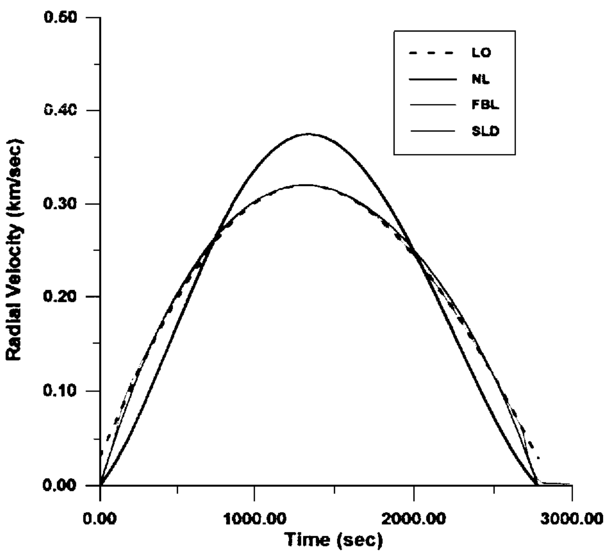

Fig. 7 Time histories of radial velocity.

The same procedure was applied to the maneuver for apogee kick firing of a communications satellite. The reference orbit was selected as the geostationary orbit. The problem was solved as an angular position-free problem by manipulating the parameters. The boundary conditions for the problem are presented in Table 4.

Table 2 presents the list of the values of parameters for the second example. The time history of total thrust acceleration has a bang–bang shape. The circumferential component of thrust acceleration has almost the same shape as that of total thrust acceleration because the radial component is very small, as shown in Fig. 8.

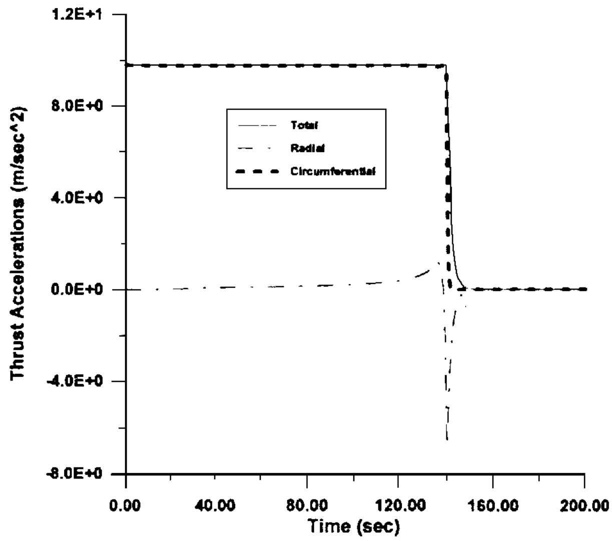

Fig. 8 Time histories of thrust accelerations.

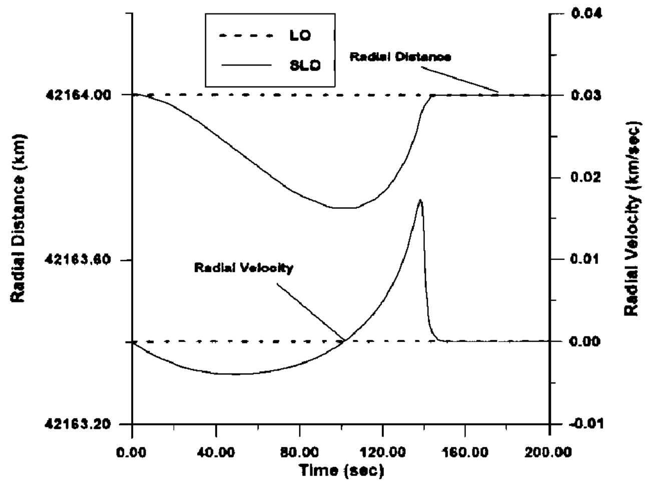

Fig. 9 Time histories of radial distance and velocity.

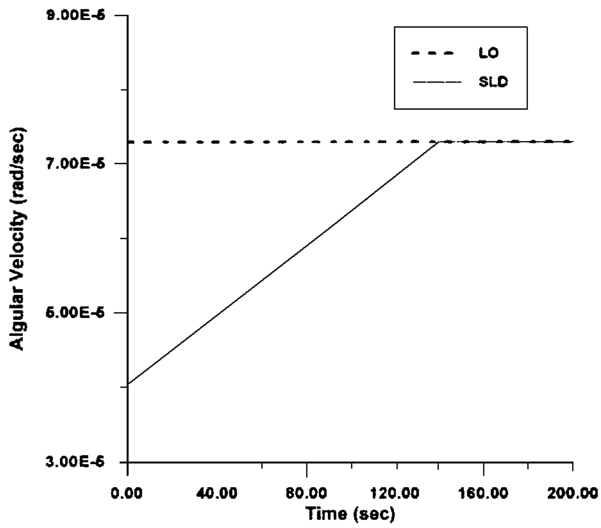

Fig. 10 Time histories of angular velocity.

Time histories of radial distance and velocity and angular velocity are presented in Figs. 9 and 10, respectively. They merge into the geostationary orbit fast and accurately. The time history of s_1 diverges at first and finally converges to zero as does the radial distance. The time history of s_2 converges to zero, as does the angular velocity (see Fig. 11).

The ΔV of Lambert's impulsive solution for the second example is 1.368 km/s and that of the bang–bang type solution using sliding

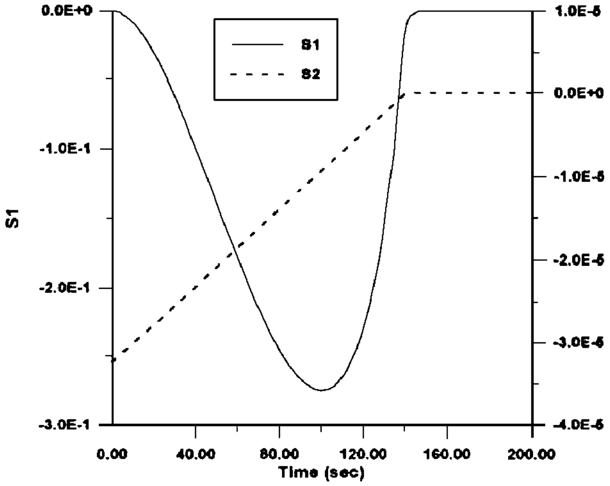

Fig. 11 Time histories of s_1 and s_2.

mode control is 1.383 km/s. Thus, the bang–bang solution is comparable to the impulsive solution to Lambert's TPBVP in terms of ΔV. In other words, the tracking is excellent.

VII. Conclusions

Bang–bang type thrust acceleration controllers for orbital maneuvers have been obtained by using a sliding mode control scheme with bounded control effort. This approach is a simple and powerful method to solve the problem defined in this paper. The total ΔV in both examples are comparable to those of respective impulsive solutions to Lambert's problem. It can account for model imprecision and perturbations even though they have not been taken into account. Feedback linearization was used to solve the same problems. Even though the solutions obtained by using feedback linearization are not bang–bang, they are still thrust-coast-thrust type solutions requiring reasonable amounts of ΔV. Applications of this approach are, of course, limited to the specific form of dynamic equations. The main benefits of the new approach are that solutions can be obtained in a very straightforward manner.

Acknowledgment

The authors appreciate the help of Sungki Cho in preparing this paper for publication.

References

[1]Lawden, D. F., *Optimal Trajectories for Space Navigation*, Butterworths Scientific, London, 1963.

[2]Kelly, H. J., "Gradient Theory of Optimal Flight Paths," *ARS Journal*, Vol. 30, No. 10, 1960, pp. 947–954.

[3]Melbourne, W. G., "Three-Dimensional Optimum Thrust Trajectories for Power Limited Propulsion Systems," *ARS Journal*, Vol. 31, Dec. 1961, pp. 1723–1728.

[4]Handelsman, M., "Optimal Free-Space Fixed-Trajectories as Starting Iteratives," *AIAA Journal*, Vol. 4, No. 6, 1966, pp. 1077–1082.

[5]Lion, P. M., Kornhauser, A. L., and Hazelrigg, G. A., Jr., "Low-Thrust Mission Analysis Using an Analytical Trajectory Optimization Model," *AIAA Journal*, Vol. 9, No. 6, 1971, pp. 1171–1175.

[6]Euler, E. A., "Optimal Low-Thrust Rendezvous Control," *AIAA Journal*, Vol. 7, No. 3, 1969, pp. 1140–1144.

[7]Tapley, B. D., and Fowler, W. T., "Terminal Guidance for Continuous Powered Space Vehicles," *AIAA Journal*, Vol. 4, No. 9, 1966, pp. 1683, 1684.

[8]McCue, G. A., "Quasilinearization Determination of Optimum Finite-Thrust Orbital Transfer," *AIAA Journal*, Vol. 5, No. 4, 1967, pp. 755–763.

[9]Lewallen, J. M., "A Modified Quasi-Linearization Method for Solving Trajectory Optimization Problems," *AIAA Journal*, Vol. 5, No. 5, 1967, pp. 962–965.

[10]Dickmanns, E. D., and Well, K. H., "Approximate Solution of Optimal Control Problems Using Third-Order Hermit Polynomial Functions," *Proceedings of the 6th Technical Conference on Optimization Techniques*, Springer–Verlag, New York, 1975 (IFIP-TC7).

[11]Hargraves, C. R., and Paris, S. W., "Direct Trajectory Optimization Using Nonlinear Programming and Collocation," *Journal of Guidance, Control, and Dynamics*, Vol. 10, No. 4, 1987, pp. 338–342.

[12]Enright, P. J., and Conway, B. A., "Optimal Finite-Thrust Spacecraft Trajectories Using Collocation and Nonlinear Programming," *Journal of Guidance, Control, and Dynamics*, Vol. 14, No. 5, 1991, pp. 981–986.

[13]Hodges, D. H., and Bless, R. R., "Weak Hamiltonian Finite Element Method for Optimal Control Problems," *Journal of Guidance, Control, and Dynamics*, Vol. 14, No. 1, 1991, pp. 148–156.

[14]Hodges, D. H., Bless, R. R., Calise, A. J., and Leung, M., "Finite Element Method for Optimal Guidance of an Advanced Launch Vehicle," *Journal of Guidance, Control, and Dynamics*, Vol. 15, No. 3, 1992, pp. 664–671.

[15]Isidori, A., Krener, A. J., Gori-Giorgi, C., and Monaco, S., "Nonlinear Decoupling via Feedback: A Differential Geometric Approach," *IEEE Transactions on Automatic Control*, Vol. AC-26, No. 2, 1981, pp. 331–345.

[16]Hunt, L. R., Su, R., and Meyer, G., "Global Transformations of Nonlinear Systems," *IEEE Transactions on Automatic Control*, Vol. AC-28, No. 1, 1983, pp. 24–30.

[17]Krener, A., "On the Equivalence of Control Systems and the Linearization of Nonlinear Systems," *SIAM Journal on Control*, Vol. 11, No. 4, 1973, pp. 670–677.

[18]Meyer, G., Su, R., and Hunt, L. R., "Application of Nonlinear Transformations to Automatic Flight Control," *Automatica*, Vol. 20, No. 1, 1984, pp. 103–107.

[19]Dwyer, T. A., III, "Exact Nonlinear Control of Large Angle Rotation Maneuvers," *IEEE Transactions on Automatic Control*, Vol. AC-29, No. 9, 1984, pp. 769–774.

[20]Dwyer, T. A., III, "Exact Nonlinear Control of Large Spacecraft Slewing Maneuvers with Internal Momentum Transfer," *Journal of Guidance, Control, and Dynamics*, Vol. 9, No. 2, 1986, pp. 240–247.

[21]Van Buran, M. A., and Mease, K. D., "Aerospace Plane Guidance Using Time-Scale Decomposition and Feedback Linearization," *Journal of Guidance, Control, and Dynamics*, Vol. 15, No. 5, 1992, pp. 1165–1174.

[22]Lee, S., "Orbital Maneuvers by Using Feedback Linearization Method," *Proceeding of Korea Automatic Control Conference*, Korea Automatic Control Conference, Seoul, Republic of Korea, 1993, pp. 480–485.

[23]Battin, R. H., *An Introduction to the Mathematics and Methods of Astrodynamics*, AIAA, New York, 1987.

[24]Filippov, A. F., "Differential Equations with Discontinuous Right-Hand Sides," *Mathematicheskii Sbornik*, Vol. 51, No. 1, 1961 (in Russian); English Translation, *Am. Math. Soc. Trans.*, Vol. 62, No. 199, 1964.

[25]Slotine, J. E., and Li, W., *Applied Nonlinear Control*, Prentice–Hall, Englewood Cliffs, NJ, 1991, Chaps. 6 and 7.

[26]Isidori, A., *Nonlinear Control Systems, An Introduction*, 2nd ed., Communications and Control Engineering Series, Springer–Verlag, New York, 1989.